Impact of Temperature and Non-Gaussian Statistics on Electron Transfer in Donor-Bridge-Acceptor Molecules

Morteza M. Waskasi,[†] Marshall D. Newton,[‡] and Dmitry V. Matyushov[†] [*,¶]

[†]*School of Molecular Sciences, Arizona State University, PO Box 871604, Tempe, AZ 85287-1604*

[‡]*Brookhaven National Laboratory, Chemistry Department, Box 5000, Upton, NY 11973-5000, United States*

[¶]*Department of Physics, Arizona State University, PO Box 871504, Tempe, AZ 85287-1504*

E-mail: dmitrym@asu.edu

Abstract

A combination of experimental data and theoretical analysis provides evidence of a bell-shaped kinetics of electron transfer in the Arrhenius coordinates $\ln k$ vs $1/T$. This kinetic law is a temperature analog of the familiar Marcus bell-shaped dependence based on $\ln k$ vs the reaction free energy. These results were obtained for reactions of intramolecular charge shift between the donor and acceptor separated by a rigid spacer studied experimentally by Miller and co-workers. The non-Arrhenius kinetic law is a direct consequence of the solvent reorganization energy and reaction driving force changing approximately as hyperbolic functions with temperature. The reorganization energy decreases and the driving force increases when temperature is increased. The point of equality between them marks the maximum of the activationless reaction rate. Reaching the consistency between the kinetic and thermodynamic experimental data requires the non-Gaussian statistics of the donor-acceptor energy gap described by the Q-model of electron transfer. The theoretical formalism combines the vibrational envelope of quantum vibronic transitions with the Q-model describing the classical component of the Franck-Condon factor and a microscopic solvation model of the solvent reorganization energy and the reaction free energy.

Keywords: Electron transfer, bell-shaped kinetic law, Arrhenius coordinates, polar solvation

Introduction

The Marcus theory of electron transfer[1] has predicted the existence of the inverted region, i.e., a drop of the rate for exoergic reactions, which occurs after reaching the maximum rate with zero activation barrier. This prediction was experimentally verified by Miller, Calcaterra, and Closs for a series of donor-spacer-acceptor molecules in which an increasingly negative reaction free energy drove the reaction from the normal region, through the maximum activationless rate, and into the inverted region.[2] Eight different acceptors were used in that study to map the entire bell-shaped Marcus energy gap law.

This pioneering work was followed by a large body of experimental evidence supporting the Marcus prediction.[3–5] Most of these studies followed the protocol set up by Miller and co-workers,[2,6,7] in which the reaction free energy, or the driving force (the negative of the reaction free energy, $-\Delta G_0$), was altered in a set of chemically modified donor-acceptor complexes. A potential drawback of this strategy is that it assumes that the rest of the parameters affecting the reaction rate (the solvent reorganization energy, electronic coupling, internal reorganization energy, and the frequency of intramolecular vibrations) remain unchanged when chemical modification is introduced. It is not easy to establish the limits of this approximation since most of these parameters are not directly accessible to experimental measurements. Despite potential limitations, this approach has been widely adopted as a way of "measuring" the reorganization energy by fitting the kinetic parameters to the Marcus energy gap law and locating the top of the "inverted parabola" at which the reorganization energy λ is equal to the driving force $-\Delta G_0$.

Additional experimental data, temperature-dependent kinetics[8,9] among them, have been accumulated to test the overall consistency of the theory. Changing the thermodynamic state of the system has offered a potentially cleaner approach to sampling the bell-shaped energy gap law since neither chemical modification of the donor-acceptor complex nor the change of the solvent[10] are involved. Pressure[11] or temperature[12,13] can be used to reach the top activationless rate and turn into the inverted region. While the assumption of molecule-independent rate parameters can be avoided in this approach, one still needs to know how the solvent reorganization energy and the driving force change when pressure and temperature are varied. Effective modeling of the dependence of the activation free energy on thermodynamic variables becomes a significant component of this research agenda.

Fitting kinetics to the energy gap law is not the only approach to access the reorganization energy experimentally. An alternative route is offered by spectroscopy of charge-transfer optical transitions,[14,15] either through direct measurement of the Stokes shift between the absorption and emission lines[16–18] or by performing the band-shape

analysis.[19–21] Measurements of the Stokes shift of charge-transfer transitions at different temperatures[17,22] have shown that the reorganization energy depends on temperature much stronger than anticipated from dielectric continuum models typically adopted in evaluating λ by the Marcus equation.[23] This general result is a consequence of the liquid state of a polar molecular solvent, producing more structural fluctuations and distinct modes of thermal agitation[12,24,25] than allowed by continuum models better suited for modeling solids. This observation, now well supported by both experiment[17,22,26,27] and numerical simulations,[25,28] calls for a critical re-examination of the early temperature-dependent kinetic data.[8,9] Those were mostly viewed as fully consistent with the Marcus picture,[8] although some inconsistencies have been identified. In particular, the reorganization energy found from fitting the kinetics to the energy gap law for Miller's set of donor-acceptor complexes fell significantly below the continuum Marcus equation.[29] Such observations, even though scarce, add to the obvious concern that if the temperature slope of the reorganization energy is significantly underestimated by continuum models,[12,24,25] a measurable deviation from the continuum prediction should be achieved in experiments performed in a sufficiently broad range of temperatures. 2-methyltetrahydrofuran (MTHF) as a solvent provides exactly this opportunity. We have taken an advantage of it here by looking at both the general problem of how temperature affects the electron transfer rate and how the individual parameters entering the rate are affected by temperature.

The standard framework to understand the effect of temperature on the reaction rate is provided by the Arrhenius law, which predicts a straight line for the rate plotted in the Arrhenius coordinates $\ln k(T)$ vs $1/T$. Although many of such data have been analyzed in the literature, the functional simplicity of the law does not allow to clearly discriminate between different theories addressing the effect of the thermodynamic state of the thermal bath on the activation barrier. The situation changes near the top of the Marcus "inverted parabola", where entropic effects become sufficiently strong to cause curved forms of $\ln k(T)$ vs $1/T$.[12] Although the experimental resolution is often insufficient, the donor-acceptor complexes from Miller's set near the top of the bell-shaped energy gap law are good candidates for observing non-trivial temperature effects. We therefore have chosen three such ASB complexes studied in the past.[9] In these molecules, a 4-biphenylyl (B) donor is connected through 5α-androstane spacer (S) to the acceptor (A). Three acceptors from Miller's set were studied here: 2-naphthyl (N), 2-benzoquinonyl (Q), and 5-chloro-2-benzoquinonyl (ClQ) (Figure 1). We have applied the microscopic solvation model[24,30] to analyze the temperature-dependent kinetics of the rate and have reached a good agreement between the theory and experiment. Based on our calculations, we have extended the range of temperatures reported in the literatures (from 179 to 373 K in MTHF[9]) and found that the rate constant, plotted in the Arrhenius coordinates, shows a bell-shaped form. This novel phenomenology is a direct consequence of a strong, nearly hyperbolic, variation of the solvation free energies entering the activation barrier with temperature.[12] To ascertain whether the experimental kinetics displays this form would require data for somewhat lower temperatures.

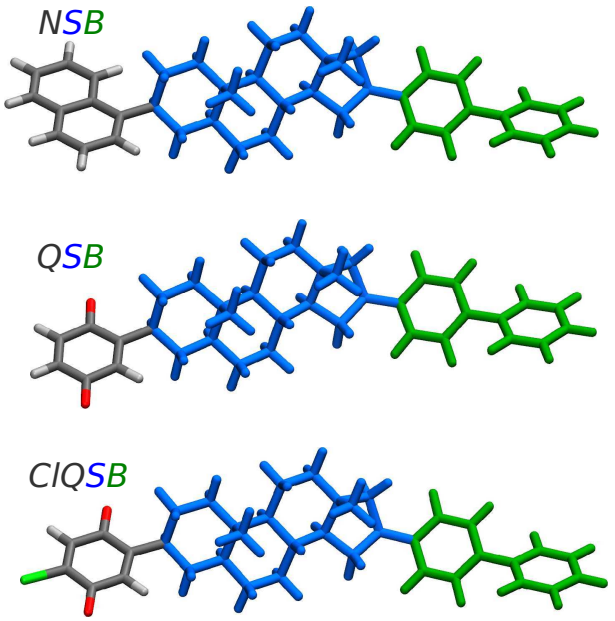

Figure 1: Structures of ASB complexes, where the anion 4-biphenylyl (B, colored green) is the donor of the electron in the electron shift through the spacer 5α-androstane (S, colored blue) to the acceptor (A, colored grey). Complexes with three acceptors from Miller's set[2] were studied here: 2-naphthyl (N), 2-benzoquinonyl (Q), and 5-chloro-2-benzoquinonyl (ClQ).

The main agenda of this study is illustrated in Figure 2. It shows fits of the experimental

rates (points) for two out of three ASB complexes displayed in Figure 1 to theoretical calculations (solid lines). Curved form of the temperature law requires taking a full account of the temperature dependence of the activation free energy and cannot be produced by assuming temperature-independent enthalpy and entropy of activation, as is commonly done in applying the Arrhenius law. Further, the dielectric continuum theories neither describe the experimental reaction free energies (see below) nor produce curved temperature laws.

The third complex, NSB does not show a curved temperature law. The experimental activation enthalpy is positive,[9] in contrast to negative (ClQSB) or rather small (QSB, but with uncertain sign and magnitude due to the error bars) activation enthalpies observed experimentally for two other complexes (Figure 2). This complex, however, presents us with an opportunity to test the consistency of the widely used combination of the Gaussian Marcus model with the Bixon-Jortner equation modeling the effect of intramolecular quantum vibrations on the reaction rate.[31] The additional source of information is provided by the temperature dependence of the reaction free energy $\Delta G_0(T)$ measured in an independent experiment.[7,8] We have found that two levels of the theory improvement are required. First, the use of the dielectric models for the solvation components of that activation barrier is inconsistent with the experimental results. One has to replace the dielectric continuum with microscopic models of solvation. Such improved theory still preserves the Gaussian statistics of the donor-acceptor energy gap and will be labeled as "Marcus theory" here. However, this improvement is not sufficient since its application to the experimental data produced parameters incompatible with experimental $\Delta G_0(T)$. At the second level of the theory improvement, we have found that replacing the Gaussian statistics of the donor-acceptor energy gap with the non-Gaussian statistics described by the Q-model of electron transfer[32,33] has eliminated the difficulty and produced consistent sets of model parameters.

The Q-model was designed to describe electron transfer reactions characterized by non-Gaussian statistics of the donor-acceptor energy gap.[32] Several physical scenarios can be identified which require this extension of the Gaussian Marcus theory. Among them are polarizable donor-acceptor com-

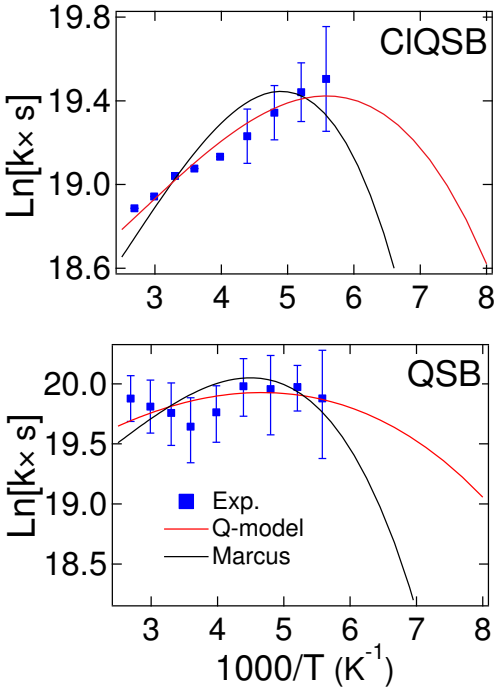

Figure 2: Rate constants in the Arrhenius coordinates ($k(T)$ vs $1/T$) for ClQSB (top) and QSB (bottom) in MTHF. The points represent experimental data[9] and the solid lines refer to the theoretical calculations combining the Franck-Condon analysis with the SolvMol[30,34] calculations of the solvent reorganization energy $\lambda(T)$ and the solvent component of the reaction Gibbs energy $\Delta G_s(T)$. The Marcus model (solid black lines) and the Q-model (solid red lines), both combined with the microscopic solvation calculations, were used to model the classical component of the Franck-Condon factor entering the rate of nonadiabatic electron transfer (eq 5). The gas-phase component of the energy gap ΔE_g (eq 13) and the electron-transfer coupling V are the fitting parameters listed in Table 1. The combination of the Gaussian statistics of the donor-acceptor energy gap with microscopic solvation models is labeled as "Marcus model" here.

plexes, in which electron transfer causes not only the change in the charge distribution, but also a change in the polarizability of the complex.[20,33,35] Other scenarios include nonlinear solvation and a coupling between classical intramolecular modes, such as torsional rotations, with the solvent polarization.[32] Both effects, polarizability and torsional rotations, potentially affect electron transfer in the ASB complexes studied here. The application of the Q-model to all three complexes (red lines in Figure 2) produce consistently superior results compared to the Gaussian Marcus model (black lines in Figure 2).

Conceptual framework

Reaction rate. The conceptual basis of the Marcus theory of electron transfer reactions goes back to Onsager's principle of microscopic reversibility.[36,37] It states that the average regression of spontaneous fluctuations obeys the same laws as the corresponding irreversible process. What this practically means is that one can calculate the reversible work[38] (free energy) required to drive the system from equilibrium to a given non-equilibrium state and that free energy will quantify the probability of the system to reach the same state by a spontaneous fluctuation driven by thermal agitation. The two properties, the probability P and the free energy F, are connected by the Gibbs distribution, $P \propto \exp[-\beta F]$, $\beta = 1/(k_{\mathrm{B}}T)$. Note that the Gibbs distribution is defined in terms of the Helmholtz free energy F, which gives the maximum reversible work gained at constant volume. In contrast, the Gibbs energy $G = F + pV$ quantifies the work done at constant pressure p. The pV term can be neglected for most problems dealing with condensed materials. We therefore use G throughout the paper, with the provision that F in fact follows from theoretical derivations using statistical mechanics.

The Marcus theory makes full use of microscopic reversibility by calculating the probability of spontaneously reaching the top of the activation barrier $\Delta G^{\dagger}$, required for kinetics, as the reversible free energy invested to drive the system to the corresponding non-equilibrium state.[1] The reasoning of microscopic reversibility also largely determines the language used by practitioners in the field, who draw their ideas from either the statistics of stochastic fluctuations or from reversible thermodynamics. Both views are indeed helpful, particularly when microscopic models of electron transfer are developed.[12,39] Fluctuations tell the mechanistic story of what are the molecular motions involved in the activation events, while equilibrium thermodynamics addresses the question of how the rates are affected by changing the thermodynamic state of the system. We will follow this traditional dual view of the problem when addressing the questions of how temperature and the statistics of fluctuations affect the rate of electron transfer.

The departure point is the definition of the reaction coordinate of electron transfer. Modern theories, following Warshel,[40] use the energy gap between the acceptor and donor electronic states of the transferred electron as the reaction coordinate X.[32,41,42] The probability to find a given value of the gap, due to a spontaneous fluctuation in the medium, is a Gaussian function,

$$P_G(X) = \left[2\pi\sigma_X^2\right]^{-1/2} e^{-(X-X_0)^2/2\sigma_X^2} \qquad (1)$$

The average energy gap $X_0 = \lambda + \Delta G_0$ is given in the Marcus theory in terms of the reorganization energy λ and the reaction free energy ΔG_0. The reorganization energy also enters the variance of the energy gap

$$\sigma_X^2 = \langle (X - X_0)^2 \rangle = 2k_{\mathrm{B}}T\lambda \qquad (2)$$

The probability distribution follows one of the dual views on the problem of electron transfer mentioned above, the fluctuation approach. The probability $P_G(0)$ of reaching the transition state $X = 0$ when electron tunneling becomes possible defines the free energy of activation

$$\Delta G^{\dagger} = \frac{X_0^2}{2\beta\sigma_X^2} = \frac{(\lambda + \Delta G_0)^2}{4\lambda} \qquad (3)$$

This probability is a factor in the Golden Rule, or non-adiabatic, rate of electron transfer[43,44]

$$k_{\mathrm{ET}} \propto V^2 P_G(0) \qquad (4)$$

where V is the electron transfer coupling. Quantum vibrations modify the picture, particularly in the inverted region of electron transfer ($X_0 < 0$). Vibrations of the donor-acceptor complex add a separate vibronic channel to each vibrational excitation with the energy $m\hbar\omega_v$. This energy is added to X_0 as $X_0 \to X_0 + m\hbar\omega_v$. In the inverted region with $X_0 < 0$, adding positive $m\hbar\omega_v$ leads to

a lower barrier in eq 3. The amplitude of each vibronic channel is determined by the corresponding Franck-Condon factor and the final result for the rate constant is given by the Bixon-Jortner expression[31]

$$k_{\rm ET} = \frac{2\pi}{\hbar} V^2 e^{-S} \sum_{m\geq 0} \frac{S^m}{m!} P_G(-m\hbar\omega_v) \qquad (5)$$

Here, $S = \lambda_v/\hbar\omega_v$ is the Huang-Rhys factor and λ_v is the reorganization energy of quantum vibrations with the characteristic frequency ω_v. Equation 3 for the activation barrier sets the position of the activationless transition, $\Delta G\dagger = 0$, at $-\Delta G_0^{\rm max} = \lambda$. This condition is modified by intramolecular vibrations and the maximum of the rate shifts to

$$-\Delta G_0^{\rm max} \simeq \lambda + \lambda_v \qquad (6)$$

The reorganization energy λ in eq 2 incorporates all classical modes affecting the donor-acceptor energy gap, which typically include the solvent modes and classical intramolecular vibrations. For organic complexes studied here, quantum intramolecular vibrations with frequencies $\hbar\omega_v^j > 2k_{\rm B}T$ dominate in the reorganization energy of intramolecular vibrations $\lambda_v = \sum_j \lambda_v^j$ (see below). The latter is a sum of contributions λ_v^j from all normal modes of vibration with the frequencies ω_v^j. In the approach adopted here, we replace the manifold of intramolecular quantum vibrations with an effective vibrational frequency[24] $\omega_v = \sum_j \omega_v^j(\lambda_v^j/\lambda_v)$. The definition of individual normal-mode components λ_v^j require resonance Raman spectroscopy.[45] In the absence of such data for the donor-acceptor molecules studied here, a generic frequency of $\omega_v = 1500$ cm^{-1} is used, as is typically assigned to organic charge-transfer complexes.[31]

In the present calculations, λ in eq 2 is assigned to the solvent reorganization energy λ_s and the former symbol is used throughout below. An alternative approach would involve identifying classical normal modes within the donor-acceptor complex and combining them with λ_s in the total classical reorganization energy λ. This approach causes significant difficulties, both computational and fundamental. The calculation of the reorganization energy components of separate normal modes is computationally challenging compared to the calculation of the overall vibrational reorganization energy achieved in terms of average gas-phase vertical energies of the complex in two charge-transfer states (see the supporting Information (SI)). A noticeable reorganization energy of $\lambda_\phi \simeq 0.13$ eV was previously assigned to the torsional rotation of the benzene rings in 4-biphenyl upon electron transfer.[46] Our calculations produce a close number of $\lambda_\phi \simeq 0.12$ eV (see SI). This rotation does not, however, correspond to a normal mode of the donor-acceptor complex and cannot be separated from the overall reorganization energy without accounting for cross coupling to all normal modes of the molecule and the solvent.

Q-Model. The cross coupling to the solvent might potentially be the most significant qualitative effect of torsional flexibility, coupled to charge transfer, in the molecules considered here and potentially other charge-transfer complexes.[47,48] Intramolecular torsional motions alter the electric field of the solute charges, thus providing a coupling mechanism between the torsional mobility and the solvent polarization.[49] When such coupling is introduced into the model of electron transfer, it results in a linear-quadratic dependence of the donor-acceptor energy gap on the solvent polarization.[32] Only a linear dependence of the energy gap on the solvent polarization is considered in the Marcus model; the extension to the linear-quadratic dependence is covered by the Q-model of electron transfer.[32]

The linear Marcus model results in a Gaussian distribution for the energy gap X (eq 1). This statistics is well satisfied when the solute-solvent coupling is established through the Coulomb interaction of the solute charges with the solvent dipoles.[50] The wave function of the solute is fixed in each state in this approximation and is not deformed by the fluctuations of the thermal bath. This is generally not correct since the wave function is obviously deformable and any molecular system is electronically polarizable. The first-order perturbation correction to the zeroth-order nondeformable wave function, accounting for the solute polarizability, leads to a self-polarization term in the energy gap changing quadratically with the electrostatic field of the solvent. Combined with the standard linear coupling between fixed charges and the solvent polarization, it leads, like in the case of torsional mobility, to a linear-quadratic dependence of the energy gap on the solvent polarization.

Both solvent-coupled torsional mobility and varying polarizability result in the linear-quadratic dependence of the energy gap on the solvent coor-

dinates and the corresponding non-Gaussian statistics of the energy gap.[20,32,33] It is likely that both of these factors are influencing the statistics of the energy gap in the complexes considered here. The Q-model provides a closed-form solution for all such problems in terms of the standard parameters of the Marcus theory and an additional parameter α quantifying the deviation from the Gaussian statistics

$$P_Q(X) = \beta A \sqrt{\frac{\lambda\alpha^3}{|X-X^*|}} e^{-\beta(\alpha|X-X^*|+\alpha^2\lambda)} I_1(2\beta\sqrt{\alpha^3\lambda|X-X^*|}) \quad (7)$$

The parameter α can be either positive or negative. In order to simplify the equations, we assume $\alpha > 0$ for most of the discussion below. Further, the normalization constant $A = (1-\exp[-\beta\alpha^2\lambda])^{-1}$ in eq 7 can be omitted in most cases and $I_1(x)$ is the modified Bessel function of the first order.[51]

The distribution of the energy gap in the Q-model is based on three parameters, instead of two parameters in the Gaussian distribution in eq 1. In addition to λ and ΔG_0, the Q-model introduces the non-Gaussian parameter α. It can be determined by combining λ, as defined by the variance of the energy gap in eq 2, with the reorganization energy $\lambda^{\rm St} = |X_{01} - X_{02}|/2$ obtained from the average energy gaps in the initial, X_{01}, and final, X_{02}, states. This reorganization energy is equal to half of the Stokes shift[16,20] associated with charge transfer (see also eq 22 below). In the Gaussian Marcus model either definition gives the same result, $\lambda^{\rm St} = \lambda$, but this equality breaks down for a non-Gaussian statistics of the energy gap. The deviation between λ and $\lambda^{\rm St}$ allows one to determine α (eq 22).

The non-Gaussian statistics of the energy gap also leads to the asymmetry of the solvent reorganization energies between the forward and backward reactions. If $\lambda = \lambda_1$ as defined by eq 2 specifies the reorganization energy of the forward reaction, then the reorganization energy of the backward reaction is given by an analogous relation, $\lambda_2 = (\beta/2)\langle(\delta X)^2\rangle_2$, $\delta X = X - X_{02}$, in which the average is now taken over the statistics of the thermal bath in the final state of the donor-acceptor complex. The reorganization energies λ_2 and λ can be related in terms of the parameter α as follows: $\lambda_2 = \lambda\alpha^3/(1+\alpha)^3$.

To summarize, any pair of reorganization energies out of three, $\lambda^{\rm St}$, λ_1, λ_2, provides the value of α. The three parameters of the model specify the activation barrier along the reaction coordinate X, which replaces eq 3 of the Marcus model with the relation

$$\Delta G^\dagger = \alpha(\sqrt{|\lambda\alpha^2/(1+\alpha) - \Delta G_0|} - \sqrt{\alpha\lambda})^2 \quad (8)$$

The Marcus theory and the Gaussian distribution in eq 1 are restored at $\alpha \to \infty$, when $\lambda^{\rm St} = \lambda_1 = \lambda_2$. One arrives at eq 3 from eq 8 in that limit, as can be shown trough a Taylor expansion performed in terms of $1/\alpha$ in eq 8.

The parameter X^* in eq 7 specifies the lowest magnitude of the energy gap, the "fluctuation boundary", allowed in the Q-model. The probability of reaching $X < X^*$ (when $\alpha > 0$ as assumed in eq 7) is identically zero, $P_Q(X) = 0$. The fluctuation boundary is given in terms of λ and ΔG_0 as $X^* = \Delta G_0 - \alpha^2\lambda/(1+\alpha)$. Note that the only restriction on the magnitude of α is to fall outside the range $-1 < \alpha < 0$ of mechanical instability.[32] For negative values of α, one has to take its absolute magnitude, $\alpha \to |\alpha|$ in eqs 7 and 8. The condition $X > X^*$ at $\alpha > 0$ changes to $X < X^*$ at $\alpha < 0$.

The extension of the Q-model to transitions involving intramolecular vibrational excitations is straightforward. One needs to replace the Gaussian distribution $P_G(-m\hbar\omega_v)$ with $P_Q(-m\hbar\omega_v)$ in eq 5. One of significant consequences of changing the statistics of the energy gap fluctuations is the shift of the position of the maximum of the rate from the one given by eq 6 to

$$-\Delta G_0^{\max} \simeq (\lambda + \lambda_v)\frac{\alpha}{1+\alpha} \underset{\alpha\to 0}{\longrightarrow} 0 \quad (9)$$

The significance of this result is that the maximum rate at the top of the Marcus bell-shaped energy gap law can be achieved at a substantially lower driving force when α becomes small (see below).

Temperature effect. As is clear from eq 2, the reorganization energy entering both the Marcus theory and the Q-model is determined by the variance of the donor-acceptor energy gap, i.e., by the breadth of thermal fluctuations modulating the gap. The fact that the thermal noise is enhanced with increasing temperature is known as the Nyquist theorem[52] and is reflected in the temperature factor in front of λ in eq 2. The question we consider next is whether λ should be treated as a temperature-independent coefficient or as carry-

ing its own dependence on temperature.

This question can be addressed by first noting that the solvent reorganization energy is identified in the Marcus theory with the free energy of polarizing the continuum dielectric representing the solvent. The notion of free energy already requires one to pay attention to possible effects of changing temperature. However, those are usually small in the continuum model and can often be neglected (see below). They arise from the Pekar factor $c_0(T)$, which is a combination of the refractive index $n(T)$ and the dielectric constant $\epsilon_s(T)$, $c_0(T) = n(T)^{-2} - \epsilon_s(T)^{-1}$. As λ is proportional to c_0 in the Marcus theory, $\lambda(T) \propto c_0(T)$, all effects of temperature on λ come from two dielectric constants, $\epsilon_\infty = n^2$ and ϵ_s.

This physical picture changes substantially when the continuum dielectric is replaced with a liquid of molecules carrying dipoles.[12,39] Thermal agitation now translates into fluctuations of dipolar orientations and dipolar positions (density). The difference between these two modes can be appreciated by turning again to Onsager's microscopic reversibility. A spontaneous rise of a fluctuation of orientations of molecular dipoles can be viewed as a reversible work invested in rotating the dipoles against the field of the donor-acceptor complex. This work will mostly require an input of energy. If one instead considers a fluctuation of molecular density, it will require rearranging the molecules against their repulsive cores, i.e., a local re-packing of the liquid. In contrast to the work invested in changing orientations, the corresponding free energy of re-packing is mostly entropic. One therefore concludes that the orientational and density fluctuations carry different thermodynamic signatures, energetic (enthalpic) for the former and entropic for the latter.

This physics displays itself directly in the liquid-state theory of electron-transfer reorganization.[12] The overall reorganization energy becomes a sum of the orientational λ_p and density components

$$\lambda = \lambda_p + \sigma_d^2/(2k_{\rm B}T), \tag{10}$$

where σ_d^2 is the variance of the energy gap produced by the density fluctuations. The reason λ is given in this form is that λ_p and σ_d^2 depend on temperature through density and are essentially constant parameters at the constant volume. When the continuum limit is taken for the solvent, which is achieved in the theory by shrinking the molecular size to zero, λ_p turns into the continuum expression and σ_d^2 vanishes. There is no density reorganization in a continuum medium and only orientations of dipoles determine λ.

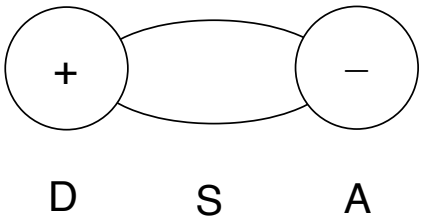

Figure 3: Schematic representation of the donor-spacer-acceptor complex. The positive hole on the donor and the negative electron on the acceptor show the "electron transfer dipole" corresponding to the difference electric field $\Delta\mathbf{E}_0$ obtained by subtracting the electric fields of the complex in the final and initial states.

The Marcus notion of the reorganization energy as the free energy of solvation might seem to have been lost in this discussion focused primarily on fluctuations. This is not correct, one just needs to turn again from the fluctuation view to the equivalent (within Onsager's paradigm) thermodynamic view. In the thermodynamic view, one considers the free energy of solvation of the "electron-transfer dipole", i.e., the difference electric field $\Delta\mathbf{E}_0 = \mathbf{E}_{02} - \mathbf{E}_{01}$ produced by the donor-acceptor complex in the acceptor, $\mathbf{E}_{02}$, and the donor, $\mathbf{E}_{01}$, states. Since the electric field of all other charges cancels out in the difference, it is effectively given by the sum of the fields of the negative electron at the acceptor and a positive hole at the donor (a dipole), as is schematically depicted in Figure 3.

In solvation theories, one can perform the perturbation expansion in terms of the interaction potential v_Δ of the electron-transfer dipole with the surrounding solvent. This is a long-ranged Coulomb interaction, while the reference system in the perturbation expansion is the repulsive core of the solute excluding the solvent from its volume through the repulsive solute-solvent interaction potential.[53] The result of the perturbation expansion is the chemical potential of solvation[54] (eq (32.3) in ref 38)

$$\mu_\Delta = \langle v_\Delta\rangle_0 - (\beta/2)\langle(\delta v_\Delta)^2\rangle_0 \tag{11}$$

where $\delta v_\Delta = v_\Delta - \langle v_\Delta\rangle_0$ and the higher order expansion terms disappear for a Gaussian medium.[54] The average $\langle\dots\rangle_0$ here is over the statistics of the medium fluctuations around the donor-acceptor

complex with v_Δ turned off, i.e., the positive and negative charges in Figure 3 removed. For most polar liquids, a repulsive molecular core of the solute carrying no charges creates no polarization in the liquid and one has $\langle v_\Delta \rangle_0 = 0$. One arrives at the equation

$$\mu_\Delta = -\lambda \tag{12}$$

implying that λ defined through the variance of the energy gap does carry the meaning of the solvation free energy according to the standard prescription of the Marcus theory. Where this prescription fails is in assigning dielectric continuum to a molecular solvent, which, being a model for a solid material, eliminates the entropic character of some of the molecular motions.[55,56]

The derivation performed above also implies that the distinct effects of the orientational and density motions of the solvent reflected in the reorganization energy should be shared by the solvent part of the reaction free energy ΔG_s. This component adds to the gas-phase energy difference ΔE_g in the overall reaction free energy ΔG_0

$$\Delta G_0 = \Delta E_g + \Delta G_s \tag{13}$$

Here, ΔE_g is the energy separation between the minima of the Born-Oppenheimer surfaces in the gas phase. It can be associated with the energy of 0-0 transition in spectroscopy.

We show below that the temperature dependence of ΔG_s essentially traces that of λ. The differences are mostly mechanistic: ΔG_s includes solvation by induced dipoles excluded from λ, and it is given by the difference in solvation chemical potentials of the final and initial states of the donor-acceptor complex, $\Delta G_s = \mu_2 - \mu_1$, instead of the chemical potential μ_Δ of the electron-transfer dipole. This observation also implies that deficiencies of the continuum dielectric in describing the temperature dependence of λ should be equally exposed in the corresponding difficulties of continuum models to describe the entropy of solvation, as is now well established.[17,55–57]

In order to connect the thermodynamic picture to the fluctuation arguments presented above, one can define the entropy of solvation

$$S_\Delta = -\left(\partial \mu_\Delta / \partial T\right)_V = -\lambda/T - \Phi/T \tag{14}$$

where the second part of this equation follows from eq 11. The term Φ in the second summand is a third-order statistical correlator,[25] $\Phi \propto \langle (\delta v_\Delta)^2 \delta H_0 \rangle$, where δH_0 is the fluctuation of the total energy of the reference system unperturbed by the Coulomb interaction of the medium with the "electron transfer dipole" (Figure 3). The term Φ is responsible for what is known in solvation theories as the "solvation reorganization energy"[58,59] (not to be confused with the electron transfer reorganization energy λ). It describes restructuring of the solvent caused by the field of the solute. Obviously, there is no restructuring in continuum models, which therefore fail to describe the solvation entropy. What is worth stressing here is a conceptual, even though not a direct mathematical, connection between "restructuring" and "density reorganization", both leading to substantial changes of λ and ΔG_s with temperature.

Rate in the Arrhenius coordinates. Equation 4 gives the reaction rate in a form formally consistent with the Arrhenius law

$$k_{\mathrm{ET}} \propto e^{-\beta \Delta G^\dagger(T)} \tag{15}$$

There is, however, an important distinction from the classical Arrhenius law,

$$k = A e^{-\beta E_a} \tag{16}$$

which assumes that the activation energy (enthalpy) E_a is constant and is given by the slope of the linear plot in the Arrhenius coordinates $\ln k$ vs $1/T$. The entropy in this simplified description enters the rate preexponent A. Since the activation energy E_a in the Arrhenius equation is associated with the height of the activation barrier in the transition state theory,[60,61] E_a has to be non-negative.

In contrast to this common view, $\Delta G^\dagger(T)$ in eqs 3 and 8 involves a fairly complex dependence on temperature arising from the solvation component of the reaction free energy $\Delta G_s(T)$ and the reorganization energy $\lambda(T)$. Both the enthalpy and entropy of activation are functions of temperature, instead of the commonly assumed constant parameters. The entropy of activation follows from $\Delta G^\dagger(T)$ as

$$\Delta S^\dagger(T) = -\left(\partial \Delta G^\dagger(T)/\partial T\right)_p \tag{17}$$

where the constant pressure conditions are applied. Correspondingly, the enthalpy of activation is

$$\Delta H^\dagger(T) = \left(\partial \beta \Delta G^\dagger(T)/\partial \beta\right)_p \tag{18}$$

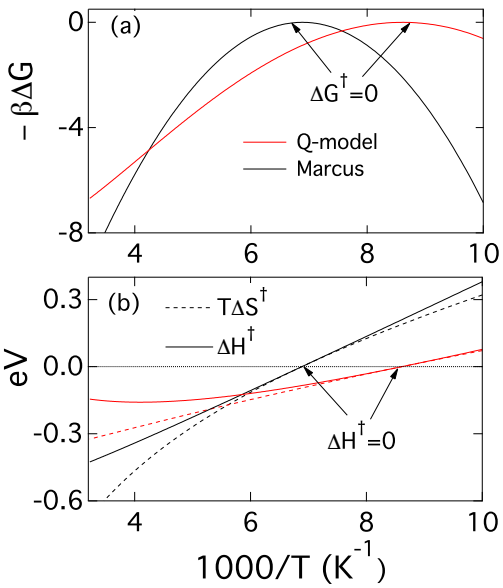

Figure 4: (a) $-\beta\Delta G^{\dagger}(T)$ and (b) $\Delta H^{\dagger}$ and $T\Delta S^{\dagger}$ vs $1/T$. Calculations are performed for the classical Marcus activation free energy in eq 3 with $\lambda(T)$ and $\Delta G_s(T)$ calculated for ClQSB complex in MTHF (Figure 1). $T\Delta S^{\dagger}(T)$ and $\Delta H^{\dagger}(T)$ are given by eqs 17 and 18, respectively. The arrows in (a) and (b) show the points of activationless electron transfer at $T = T^*$ (eqs 19 and 20) when $\Delta G^{\dagger} = \Delta H^{\dagger} = \Delta S^{\dagger} = 0$. The results of using the Marcus model for $\Delta G^{\dagger}(T)$ (eq 3) are shown in black, red marks the results of applying the Q-model (eq 8).

One therefore generally anticipates that the measured rates will be given by a curved function in the Arrhenius coordinates and the local slope $\Delta H^{\dagger}(T)$ will change in a sufficiently wide range of temperatures (Figure 4b).

This general phenomenology finds its dramatic confirmation in the bell-shaped form of the rate constant plotted in the Arrhenius coordinates as predicted theoretically[12] and observed experimentally for a number of charge-transfer systems.[13,48,62–64] While the standard, Arrhenius-type reaction kinetics is typically found for electron transfer, anti-Arrhenius portions of this overall bell-shaped temperature law have been observed in the past and discussed in terms of a negative activation enthalpy.[65–67] This feature was also reported for two out of three Miller's complexes (ClQSB and QSB in Figure 1), as is shown in Figure 2 and discussed in more detail below.

The basic phenomenology of the bell-shaped rate law is sketched in Figure 4a. This curved form of the rate law is the projection of the Marcus energy gap law on the $1/T$ coordinate.[12,68] It arises as the consequence of crossing the point $X_0(T^*) = 0$ at the temperature T^* when activationless electron transfer is reached by changing the temperature. The reorganization energy is equal to the driving force at T^*

$$-\Delta G_0(T^*) = \lambda(T^*) \tag{19}$$

in the Marcus theory. The Q-model predicts an alternative result

$$-\Delta G_0(T^*) = \alpha\lambda(T^*)/(1+\alpha) \tag{20}$$

where, as above, $\alpha > 0$ is assumed. The activation barrier is positive on both sides of T^*, but both the activation enthalpy and the activation entropy change from negative values at $T > T^*$ to positive values below T^* (Figure 4b).

Results

Here we apply the general ideas discussed above to the calculation of the rates of three complexes shown in Figure 1. All calculations have been done by using eqs 1, 5, and 7 in which the solvent reorganization energy $\lambda(T)$ and the solvent part of the reaction free energy $\Delta G_s(T)$ are calculated theoretically with the software package SolvMol.[34] This approach leaves two parameters in the rate equa-

tion unspecified, the electron-transfer coupling V and the gas-phase energy gap ΔE_g, when the Marcus model is used to describe the classical distribution of energy gaps entering the Franck-Condon factor. The use of the Q-model adds one additional parameter, α, quantifying the deviation from the Gaussian statistics. These parameters have been varied to produce best fits to experimental $k_{\rm ET}(T)$ and the results are listed in Table 1. The quality of the fits is shown in Figures 2 and 5. The vacuum energy gaps ΔE_g for all complexes have also been calculated with CDFT.[69] The accuracy of such calculations is insufficient for kinetic modeling (see SI) and fits to experimental rates are more reliable. The vibrational reorganization energies λ_v were calculated from DFT and CDFT (see SI) and are also listed in Table 1.

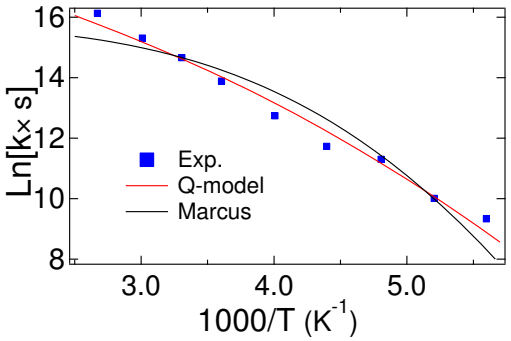

Figure 5: Rate constants in the Arrhenius coordinates ($k(T)$ vs $1/T$) for NSB in MTHF. The points represent experimental data[8] and the solid lines refer to the theoretical calculations. The black line indicates the Marcus model (eq 1) used in the Bixon-Jortner equation (eq 5), the red line refers to the Q-model (eq 7) used in eq 5. SolvMol[30,34] was used to calculate the solvent reorganization energy $\lambda(T)$ and the solvent component of the reaction Gibbs energy $\Delta G_s(T)$. The gas-phase component of the energy gap ΔE_g and the electron-transfer coupling V are the fitting parameters listed in Table 1. The parameter $\alpha = 1.14$, quantifying the non-Gaussian character of the energy gap statistics, was determined from the fit; $\alpha \to \infty$ leads to the Marcus limit with the Gaussian statistics of X.

The fits of experimental rates by using the Gaussian Marcus model in eq 5 are shown by the black solid lines in Figures 2 and 5; the fits to the Q-model are shown by the red solid lines. While the quality of the fits is consistently better in the case of the Q-model, this success can be attributed to a higher mathematical flexibility of the equations due to an additional fitting parameter α. A consistency test is required and it is provided by experimental data for the temperature dependent reaction free energy $\Delta G_0(T)$ available for the NSB complex.[7,8]

Experimental data for $\Delta G_0(T)$ of NSB were obtained from the equilibrium constant for the reaction of charge shift from biphenylyl$^-$ (B^-) to 2-naphthyl (N) group in the NSB complex in MTHF.[7,8] The measurements were a combination of BC/NC and BS/NS equilibria, where cyclohexane (C) spacer was used at low temperatures. Nevertheless the two sets of data were consistent, with nearly temperature independent free energies $\Delta G_0(T)$ (Figure 6, points), as one would anticipate if the free energy of solvation of B^- and N^- were close in the magnitude.

The main distinction between the results of fits to the Marcus theory and the Q-model comes as the magnitude of the gas-phase energy gap ΔE_g calculated from the fit of the kinetic data. The fit to the standard Marcus theory used in eq 5 leads to ΔG_0 significantly more negative than experiment (black line in Figure 6). In contrast, the fit of the kinetic data to the Q-model produces a nearly perfect agreement with the experimental $\Delta G_0(T)$ without additional fitting parameters (red line in Figure 6).

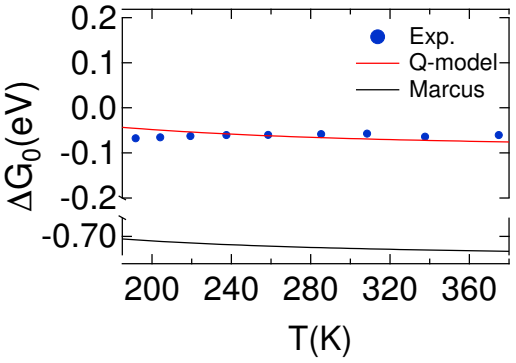

Figure 6: Temperature dependence of the reaction free energy for the NSB complex. The points are experimental data[7,8] and the solid line is the theoretical calculation combining ΔE_g from the fit of the experimental rates with ΔG_s from SolMol[30,34] (eq 13). The black solid line is obtained with ΔE_g from the fit of the experimental rates to the Marcus model (eqs 1 and 5). The red solid line refers to ΔG_0 with its gas-phase component ΔE_g obtained from fitting experimental rates with the Q-model (eqs 5 and 7).

The ability to fit the experimental kinetic data

Table 1: Parameters of electron transfer reactions (eV) at $T = 300$ K (solvation parameters refer to MTHF).

Complex	Gas			Solvent		Total
	$V \times 10^3$ [a]	λ_v [b]	ΔE_g [c]	λ [d]	ΔG_s [d]	ΔG_0 [e]
			Marcus			
NSB	0.03	0.41	-0.77	0.86	0.04	-0.73 [f]
QSB	0.22	0.50	-1.47 [g]	0.74	0.05	-1.42 [h]
ClQSB	0.16	0.49	-1.54	0.73	0.06	-1.48 [h]
			Q-model			
NSB	0.07	0.41	-0.11	0.86	0.04	-0.07 [f]
QSB	0.21	0.50	-1.06 [g]	0.74	0.05	-1.01 [h]
ClQSB	0.16	0.49	-1.27	0.73	0.06	-1.21 [h]

[a] Obtained by fitting the kinetic data for all three complexes. The application of the Q-model resulted in $\alpha = 1.14$, 1.22 and 1.74 for NSB, QSB and ClQSB, respectively. [b] The vibrational reorganization energies were calculated from the gas-phase vertical transition energies as the mean of two values, $\lambda_v = (\lambda_{v1} + \lambda_{v2})/2$, which can be produced from the gas-phase energy surfaces (DFT/B3LYP/6-31G, see Tables S1 and S2 in SI). The characteristic vibrational frequency of $\omega_v = 1500$ cm^{-1} was assigned to all complexes. [c] ΔE_g values listed in the table were obtained as fitting parameters in the analysis of the kinetic data for ASB complexes; $\Delta E_g \simeq 0$ (NSB), -2.35 eV (QSB), and -2.74 eV (ClQSB) were calculated with DFT, see Table S1 in SI. [d] Calculated by using the microscopic solvation model SolvMol. [e] From eq 13. [f] Experimental ΔG_0 in MTHF[7] is -0.06 eV at $T = 300$ K. [g] Redox potentials measured for Q and B in dimethylformamide[2] were used to estimate the gas-phase energy gap between separate fragments. SolvMol calculations of the solvation energies of Q^- and B^- combined with the experimental $\Delta G_0^{\rm redox}$ yield $\Delta E_g(\infty) = -1.68$ eV at an infinite donor-acceptor separation (see SI for more details). [h] The present calculations of ΔG_0 cannot be directly compared with those listed by Miller,[2] since they were based on the redox potentials of the isolated fragments in a different solvent (dimethylformamide).

and to obtain the bell-shaped curve in the Arrhenius coordinates (Figure 2) are greatly affected by the strong dependence of the reorganization energy on temperature predicted by the microscopic solvation model. The dielectric continuum does not capture this physics as illustrated in Figure 7, where we compare the SolvMol calculations with the dielectric model implemented in the numerical software DelPhi numerically solving the Poisson equation.[70,71] As expected, the continuum model grossly underestimates the change of the reorganization energy with temperature[24,25] (the slope of λ with increasing temperature is nearly zero in Figure 7). The microscopic and continuum results are numerically close at $T \sim 300$ K, which implies that the continuum models were empirically parametrized to reproduce solvation free energies around this temperature. However, the gross underestimate of the solvation entropy by the dielectric models[17,55–57] eventually leads to incorrect free energies in an extended range of temperatures.

The top of the bell-shaped kinetic law in the

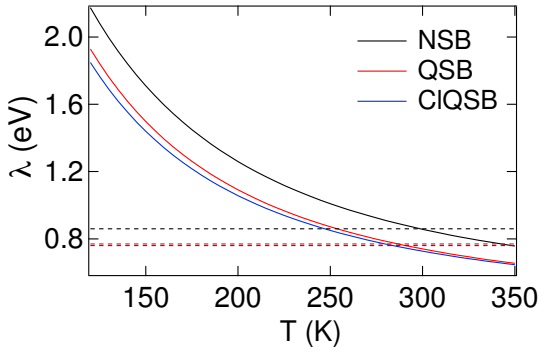

Figure 7: Solvent reorganization energy λ vs temperature for NSB (black), QSB (red), and ClQSB (blue) in MTHF. The solid lines refer to the calculations with SolvMol[30,34] (microscopic solvation model) and the dashed lines show the calculations using DelPhi[71] (continuum solvation model).

Arrhenius coordinates represents the activationless regime ($\Delta G^{\dagger}(T^*) = 0$), when the average energy gap is zero, $X_0(T^*) = 0$. The temperature dependence of the barrier arises from the solvent component of the driving force $-\Delta G_s(T)$ and the solvent reorganization energy $\lambda(T)$. The point of the maximum in the Arrhenius coordinates is their crossing point in the Marcus theory (eq 19 and Figure 8). As mentioned above, using continuum dielectric to model the solvent effect on electron transfer produces the reorganization energy nearly independent of temperature (Figure 7) and no maximum in the Arrhenius coordinates.

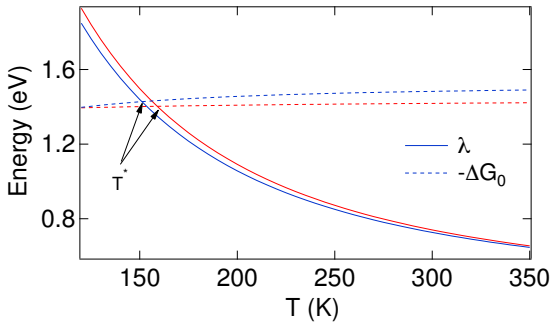

Figure 8: Temperature variation of the solvent reorganization energy $\lambda(T)$ (solid lines) and the driving force $-\Delta G_0$ (dashed lines) calculated for electron transfer in ClQSB (blue) and QSB (red) in 2-methyltetrahydrofuran (MTFH). The calculations are performed with the microscopic solvation model SolvMol.[30,34] The arrows indicate the temperature T^* at which zero activation barrier is reached in the Marcus theory of electron transfer (eq 19). The condition of maximum rate is altered in the Q-model (eq 20).

Discussion

The extraordinary predictive power of the Marcus theory[23] is based on the fundamental Gaussian statistics of the medium fluctuations projected on the one-dimensional reaction coordinate. The bell-shaped energy gap law provides the means of experimental sampling of the energy gap statistics by varying the reaction free energy.[2] When this fundamental view of thermal fluctuations in polar media is supplemented with microscopic liquid state models, the theory becomes capable of very detailed predictions of the effect of thermodynamic parameters on the reaction rate.

Electron transfer with low activation barriers brings forward entropic effects usually hidden behind the Arrhenius phenomenology. The appearance of a bell-shaped rate law in the Arrhenius coordinates ($\ln(k)$ vs $1/T$) is a dramatic consequence of such entropic effects (Figure 2). This new phenomenology provides an alternative experimental approach to sample the statistics of the donor-acceptor energy gap by varying the temperature. The ability to sample the bell-shaped rate law by varying temperature relies on a relatively strong variation of the solvation free energies entering the activation barrier. The microscopic solvation theory[12,30] suggests that the most relevant functionality for both $-\Delta G_0$ and λ is hyperbolic, $a + b/T$. The top of the bell-shaped dependence marks the point of activationless electron transfer: the reaction is in the Marcus inverted region at high temperatures and crosses to the normal region at lower temperatures.

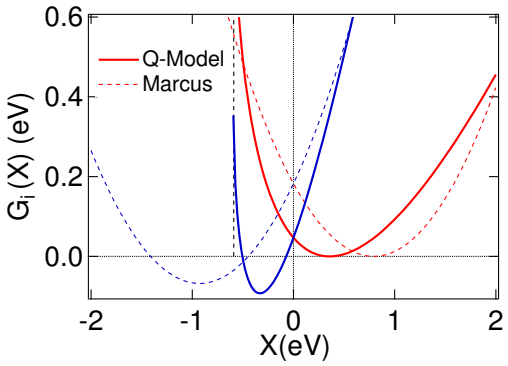

Figure 9: $G_1(X)$ (red) and $G_2(X)$ (blue) for electron transfer in the NSB complex calculated with the parameters listed in Table 1. The non-Gaussian parameter $\alpha = 1.14$ is used in the Q-model calculations (solid lines) and $\alpha \to \infty$ is set to produce the Marcus limit (dashed lines). The vertical dotted line indicates $X = 0$ at which the free energy surfaces cross and electron tunneling becomes possible. The vertical dashed line indicates the position of the "fluctuation border" X^* of the Q-model below which $G_i(X) \to \infty$. The distance between the minima of the free energy surfaces is equal to $2\lambda^{\mathrm{St}}$, where λ^{St} is the Stokes shift reorganization energy.

Gaussian statistics is not required to obtain the bell-shaped energy gap law. Already the involvement of quantum intramolecular vibrations of the donor-acceptor complex (eq 5) brings about the de-

viation of the energy gap shape from the inverted parabola of the Marcus theory.[31] Further deviations from the inverted parabola are allowed by the Q-model producing non-Gaussian statistics of the donor-acceptor energy gap.[32] However, the maximum rate at the top of the bell-shaped curve is still reached at the point of zero average energy gap, $X_0 = 0$, producing activationless electron transfer.

The Q-model brings a number of new features to the general phenomenology of electron transfer in donor-bridge-acceptor systems. First, since the fluctuations of the energy gap are not Gaussian, the free energy surfaces of electron transfer are non-parabolic. The extent of deviation from the parabolic shape is very substantial for $\alpha = 1.14 - 1.74$ following from the fits of the kinetic data (from NSB to ClQSB in Table 1). The free energy surfaces follow directly from the corresponding probabilities $P_i(X)$ as

$$G_i(X) = G_{0i} - \beta^{-1} \ln [P_i(X)] \qquad (21)$$

where $i = 1$ and $i = 2$ refer to the forward and backward reactions, respectively. Here, G_{0i} is the free energy at the minimum such that the reaction free energy is $\Delta G_0 = G_{02} - G_{01}$.

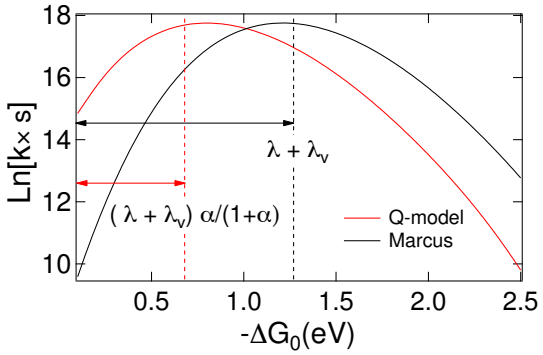

Figure 10: Energy gap law based on the Marcus model (black line) and the Q-model (red line). The parameters are for the NSB complex at $T = 300$ K as listed in Table 1.

The free energy surface resulting from the Marcus theory and the Q-model are compared in Figure 9 in the case of the NSB complex. As is clearly seen, the Q-model predicts a significant decrease of the activation barrier at a given value of the driving force $-\Delta G_0$. The rate of electron transfer can therefore be substantially increased without sacrificing the reaction free energy, a feature significant for applications to solar energy conversion.[72] Apart

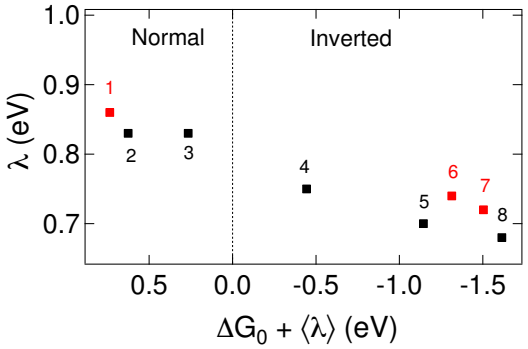

Figure 11: Solvent reorganization energies of electron transfer in Miller's set of donor-acceptor complexes.[2] The molecular charge distribution in the donor-acceptor complexes was calculated from CDFT (see SI) and was used in SolvMol[30] to calculate λ. The calculated values are plotted against $\Delta G_0 + \langle\lambda\rangle$, where $\langle\lambda\rangle$ is the average reorganization energy in the set and ΔG_0 is the experimental reaction free energy from redox potentials.[2] The complexes included in the set are of the general ASB form (Figure 1) with the following acceptors A: 2-naphthyl (1), 9-phenanthryl (2), pyrenyl (3), hexahydronaphthoquinon-2-yl (4), 2-naphthoquinonyl (5), 2-benzoquinonyl (6), 5-chlorobenzoquinon-5-yl (7), 5,6-dichlorobenzoquinon-2-yl (8). The ASB complexes shown in Figure 1 are marked red in the plot.

from the nonlinear shape of $G_i(X)$, the reduction of the barrier is achieved by reducing the distance between the minima of the free energy curves from 2λ in the Marcus theory to the value

$$2\lambda^{\mathrm{St}} = \lambda \, \frac{\alpha(1+2\alpha)}{(1+\alpha)^2} \qquad (22)$$

The reorganization energy λ^{St} refers to half of the Stokes shift between the absorption and emission maxima of charge-transfer bands.[16,20] In the Gaussian model, one has $\lambda^{\mathrm{St}} = \lambda$, as is seen from eq 22 at $\alpha \to \infty$. However, the distance between the absorption and emission maxima shrinks as α decreases.[20] In terms of thermally activated electron transfer, one has $2\lambda^{\mathrm{St}} = |X_{01} - X_{02}|$ and the same phenomenology is reflected in closer minima of the free energy surfaces and a lower activation barrier (Figure 9).

This general result is also clearly seen in the reaction energy gap law shown in Figure 10, where the fitting parameters for the NSB complex are used to compare the Marcus theory to the Q-model. Since $\alpha \simeq 1$ from our fitting, the top of the bell-shaped energy gap law, that is the maximum rate, shifts from $\simeq \lambda + \lambda_v$, per eq 6, to about half of this value ($\simeq (\lambda + \lambda_v)/2$, eq 9). Therefore, donor-acceptor complexes satisfying the rules of the Q-model (either through varying polarizability or the coupling of dihedral rotations to the solvent) achieve the maximum rate of electron transfer at the driving force significantly reduced compared to the Gaussian (Marcus) model. This observation might help in designing charge-transfer complexes for efficient solar energy conversion since fast charge separation, followed by a long-living charge separated state, is highly sought in those applications.[73–75] The broadly accepted line of thought for achieving such conditions is to perform reactions in low-polarity solvents[76–78] with a low value of λ. An alternative approach, suggested by the Q-model, would be to seek conditions for a low magnitude of the non-Gaussian parameter α.

All these mechanistic details, which are potentially important for both the fundamental understanding of electron transfer and for applications to solar energy conversion, are washed out in the standard construction of the energy gap law when $\ln(k_{\mathrm{ET}})$ is plotted vs the driving force $-\Delta G_0$ under the assumption that all other parameters of the reaction remain unchanged. The reorganization energy, which defines the top of the Marcus bell-shaped law in Miller's set of donor-acceptor complexes, turns out to be equal to 0.75 eV.[2] While this value is close to the corresponding results for QSB and ClQSB from our calculations (Table 1), this does not mean that the assumption of a constant reorganization energy within the set is well justified. The results of our calculations of λ for all eight complexes from Miller's set is shown in Figure 11 (see Table S6 in SI). It is clear that the values of λ are spread over a significant range and the assumption of a constant reorganization energy throughout the set is an approximation.

Acknowledgement This research was supported by the Office of Basic Energy Sciences, Division of Chemical Sciences, Geosciences, and Energy Biosciences, Department of Energy (DE-SC0015641). CPU time was provided by the National Science Foundation through XSEDE resources (TG-MCB080116N).

References

(1) Marcus, R. A. On the Theory of Oxidation-Reduction Reactions Involving Electron Transfer. I. *J. Chem. Phys.* **1956**, *24*, 966.

(2) Miller, J. R.; Calcaterra, L. T.; Closs, G. L. Intramolecular long-distance electron transfer in radical anions. The effects of free energy and solvent on the reaction rates. *J. Am. Chem. Soc.* **1984**, *106*, 3047–3049.

(3) Imahori, H.; Tamaki, K.; Guldi, D. M.; Luo, C.; Fujitsuka, M.; Ito, O.; Sakata, Y.; Fukuzumi, S. Modulating Charge Separation and Charge Recombination Dynamics in PorphyrinFullerene Linked Dyads and Triads: Marcus-Normal versus Inverted Region. *J. Am. Chem. Soc.* **2001**, *123*, 2607–2617.

(4) Schuster, D. I.; Cheng, P.; Jarowski, P. D.; Guldi, D. M.; Luo, C.; Echegoyen, L.; Pyo, S.; Holzwarth, A. R.; Braslavsky, S. E.; Williams, R. M. et al. Design, Synthesis, and Photophysical Studies of a Porphyrin-Fullerene Dyad with Parachute Topology; Charge Recombination in the Marcus Inverted Region. *J. Am. Chem. Soc.* **2004**, *126*, 7257–7270.

(5) Guldi, D. M. Nanometer scale carbon structures for charge-transfer systems and pho-

tovoltaic applications. *Phys. Chem. Chem. Phys.* **2007**, *9*, 1400.

(6) Closs, G. L.; Miller, J. R. Intramolecular long-distance electron transfer in organic molecules. *Science* **1988**, *240*, 440–447.

(7) Miller, J. R.; Penfield, K.; Johnson, M.; Closs, G.; Green, N. In *Photochemistry and Radiation Chemistry. Complementary methods for the study of electron transfer*; Wishart, J. F., Nocera, D. G., Eds.; Advances in Chemistry; American Chemical Society, 1998; Vol. 254; pp 161–176.

(8) Liang, N.; Miller, J. R.; Closs, G. L. Correlating temperature dependence to free-energy dependence of intramolecular long-range electron transfers. *J. Am. Chem. Soc.* **1989**, *111*, 8740–8741.

(9) Liang, N.; Miller, J. R.; Closs, G. L. Temperature-Independent Long-Range Electron-Transfer Reactions in the Marcus Inverted Region. *J. Am. Chem. Soc.* **1990**, *112*, 5353–5354.

(10) Hupp, J. T.; Dong, Y.; Blackbourn, R. L.; Lu, H. Does Marcus-Hush theory really work? The solvent dependence of intervalence charge-transfer energetics in pentaammineruthenium(II)-4,4'-bipyridine)-pentaammineruthenium(III)]5+ in the limit of infinite dilution. *J. Phys. Chem.* **1993**, *97*, 3278–3282.

(11) Holroyd, R.; Miller, J. R.; Cook, A. R.; Nishikawa, M. Pressure Tuning of Electron Attachment to Benzoquinones in Nonpolar Fluids: Continuous Adjustment of Free Energy Changes. *J. Phys. Chem. B* **2014**, *118*, 2164–2171.

(12) Matyushov, D. V. A molecular theory of electron transfer reactions in polar liquids. *Mol. Phys.* **1993**, *79*, 795.

(13) Waskasi, M. M.; Gerdenis,; Moore, A. L.; Moore, T. A.; Gust, D.; Matyushov, D. V. Marcus bell-shaped electron transfer kinetics observed in an Arrhenius plot. *J. Am. Chem. Soc.* **2016**, *138*, 9251–9257.

(14) Creutz, C.; Newton, M. D.; Sutin, N. Metal-ligand and metal-metal coupling elements. *J. Photochem. Photobiol. A: Chem.* **1994**, *82*, 47.

(15) Brunschwig, B. S.; Creutz, C.; Sutin, N. Optical transitions of symmetrical mixed-valence systems in the Class II–III transition regime. *Chem. Soc. Rev.* **2002**, *31*, 168–184.

(16) Reynolds, L.; Gardecki, J. A.; Frankland, S. J. V.; Maroncelli, M. Dipole solvation in nondipolar solvents: Experimental studies of reorganization energies and solvation dynamics. *J. Phys. Chem.* **1996**, *100*, 10337–10354.

(17) Vath, P.; Zimmt, M. B.; Matyushov, D. V.; Voth, G. A. A failure of continuum theory: Temperature dependence of the solvent reorganization energy of electron transfer in highly polar solvents. *J. Phys. Chem. B* **1999**, *103*, 9130.

(18) Sajadi, M.; Ernsting, N. P. Excess Dynamic Stokes Shift of Molecular Probes in Solution. *J. Phys. Chem. B* **2013**, *117*, 7675–7684.

(19) Gould, I. R.; Noukakis, D.; Gomes-Jahn, L.; Young, R. H.; Goodman, J. L.; Farid, S. Radiative and nonradiative electron transfer in contact radical-ion pairs. *Chem. Phys.* **1993**, *176*, 439–456.

(20) Matyushov, D. V.; Newton, M. D. Understanding the optical band shape: Coumarin-153 steady-state spectroscopy. *J. Phys. Chem. A* **2001**, *105*, 8516–8532.

(21) Levy, D.; Arnold, B. R. Analysis of Charge-Transfer Absorption and Emission Spectra on an Absolute Scale: Evaluation of Free Energies, Matrix Elements, and Reorganization Energies. *J. Phys. Chem. A* **2005**, *109*, 8572–8578.

(22) Vath, P.; Zimmt, M. B. A spectroscopic study of solvent reorganization energy: Dependence on temperature, charge transfer and the type of solute-solvent interactions. *J. Phys. Chem. A* **2000**, *104*, 2626.

(23) Marcus, R. A. On the theory of electron-transfer reactions. VI. Unified treatment for homogeneous and electrode reactions. *J. Chem. Phys.* **1965**, *43*, 679.

(24) Milischuk, A. A.; Matyushov, D. V.; Newton, M. D. Activation entropy of electron transfer reactions. *Chem. Phys.* **2006**, *324*, 172–194.

(25) Ghorai, P. K.; Matyushov, D. V. Solvent reorganization entropy of electron transfer in polar solvents. *J. Phys. Chem. A* **2006**, *110*, 8857–8863.

(26) Derr, D. L.; Elliott, C. M. Temperature dependence of the outer-sphere reorganization energy. *J. Phys. Chem. A* **1999**, *103*, 7888.

(27) Solis, C.; Grosso, V.; Faggioli, N.; Cosa, G.; Romero, M.; Previtali, C.; Montejano, H.; Chesta, C. Estimation of the solvent reorganization energy and the absolute energy of solvation of charge-transfer states from their emission spectra. *Photochem. Photobiol. Sci.* **2010**, *9*, 675–686.

(28) Wu, E. C.; Kim, H. J. MD Study of Stokes Shifts in Ionic Liquids: Temperature Dependence. *J. Phys. Chem. B* **2016**, *120*, 4644–4653.

(29) Paulson, B.; Pramod, K.; Eaton, P.; Closs, G. Long-distance electron transfer through rodlike molecules with cubyl spacers. *J. Phys. Chem.* **1993**, *97*, 13042–13045.

(30) Matyushov, D. V. Solvent reorganization energy of electron transfer in polar solvents. *J. Chem. Phys.* **2004**, *120*, 7532–7556.

(31) Bixon, M.; Jortner, J. Electron transfer – from isolated molecules to biomolecules. *Adv. Chem. Phys.* **1999**, *106*, 35.

(32) Matyushov, D. V.; Voth, G. A. Modeling the free energy surfaces of electron transfer in condensed phases. *J. Chem. Phys.* **2000**, *113*, 5413.

(33) Small, D. W.; Matyushov, D. V.; Voth, G. A. The theory of electron transfer: What may be missing? *J. Am. Chem. Soc.* **2003**, *125*, 7470–7478.

(34) SolvMol Package, Copyright ASU. 2008; `http://theochemlab.asu.edu/?q=SolvMol`.

(35) Dinpajooh, M.; Matyushov, D. V. Non-Gaussian Lineshapes and Dynamics of Time-Resolved Linear and Nonlinear (Correlation) Spectra. *J. Phys. Chem. B* **2014**, *118*, 7925–7936.

(36) Onsager, L.; Machlup, S. Fluctuations and irreversible processes. *Phys. Rev.* **1953**, *91*, 1505–1512.

(37) de Groot, S. R.; Mazur, P. *Nonequilibrium Thermodynamics*; Dover: New York, 1984.

(38) Landau, L. D.; Lifshits, E. M. *Statistical Physics*; Pergamon Press: London, 1958; Vol. V. 5 of Course of Theoretical Physics.

(39) Perng, B.-C.; Newton, M. D.; Raineri, F. O.; Friedman, H. L. Energetics of charge transfer reactions in solvents of dipolar and higher order multipolar character. II. Results. *J. Chem. Phys.* **1996**, *104*, 7177.

(40) Warshel, A. Dynamics of reactions in polar solvents. Semiclassical trajectory studies of electron-transfer and proton-transfer reactions. *J. Phys. Chem.* **1982**, *86*, 2218–2224.

(41) Zusman, L. D. Outer-sphere electron transfer in polar solvents. *Chem. Phys.* **1980**, *49*, 295–304.

(42) Blumberger, J.; Sprik, M. Quantum vs classical electron transfer energy as reaction coordinate for the aqueous Ru^{2+}/Ru^{3+} redox reaction. *Theor. Chem. Acc.* **2006**, *115*, 113–126.

(43) Barbara, P. F.; Meyer, T. J.; Ratner, M. A. Contemporary issues in electron transfer research. *J. Phys. Chem.* **1996**, *100*, 13148–13168.

(44) Newton, M. D. Control of electron transfer kinetics: Models for medium reorganization and donor-acceptor coupling. *Adv. Chem. Phys.* **1999**, *106*, 303.

(45) Valverde-Aguilar, G.; Wang, X.; Nelsen, S. F.; Zink, J. I. Photoinduced Electron Transfer in 2- tert-Butyl-3-(Anthracen-9-yl)-2,3-Diazabicyclo[2.2.2]octane. *J. Am. Chem. Soc.* **2006**, *128*, 6180–6185.

(46) Miller, J. R.; Paulson, B. P.; Bal, R. Torsional low-frequency reorganization energy of biphenyl anion in electron transfer reactions. *J. Phys. Chem.* **1995**, *99*, 6923–6925.

(47) Davis, W. B.; Svec, W. A.; Ratner, M. A.; Wasielewski, M. R. Molecular-wire behaviour in p-phenylenevinylene oligomers. *Nature* **1998**, *396*, 60–63.

(48) Davis, W. B.; Ratner, M. A.; Wasielewski, M. R. Conformational gating of long distance electron transfer through wire-like bridges in donor-bridge-acceptor molecules. *J. Am. Chem. Soc.* **2001**, *123*, 7877.

(49) Kirin, D. Torsional frequency of biphenyl molecule. *J. Phys. Chem.* **1988**, *92*, 3691–3692.

(50) Kuharski, R. A.; Bader, J. S.; Chandler, D.; Sprik, M.; Klein, M. L.; Impey, R. W. Molecular model for aqueous ferrous-ferric electron transfer. *J. Chem. Phys.* **1988**, *89*, 3248–3257.

(51) Abramowitz, M., Stegun, I. A., Eds. *Handbook of Mathematical Functions*; Dover: New York, 1972.

(52) Kubo, R. The fluctuation-dissipation theorem. *Rep. Prog. Phys.* **1966**, *29*, 255–284.

(53) Hansen, J. P.; McDonald, I. R. *Theory of Simple Liquids*; Academic Press: Amsterdam, 2003.

(54) Hummer, G.; Pratt, L. R.; Garcia, A. E. Free Energy of Ionic Hydration. *J. Phys. Chem.* **1996**, *100*, 1206–1215.

(55) Roux, B.; Yu, H.-A.; Karplus, M. Molecular basis for the Born model of ion solvation. *J. Phys. Chem.* **1990**, *94*, 4683.

(56) Lynden-Bell, R. M.; Rasaiah, J. C. From hydrophobic to hydrophilic behaviour: A simulation study of solvation entropy and free energy of simple solutes. *J. Chem. Phys.* **1997**, *107*, 1981–1991.

(57) LeBard, D. N.; Matyushov, D. V. Redox Entropy of Plastocyanin: Developing a Microscopic View of Mesoscopic Solvation. *J. Chem. Phys.* **2008**, *128*, 155106.

(58) Yu, H.-A.; Karplus, M. A thermodynamic analysis of solvation. *J. Chem. Phys.* **1988**, *89*, 2366.

(59) Guillot, B.; Guissani, Y. A computer simulation study of the temperature dependence of the hydrophobic hydration. *J. Chem. Phys.* **1993**, *99*, 8075–8094.

(60) Eyring, H.; Lin, S. H.; Lin., S. M. *Basic Chemical Kinetics*; Wiley-Interscience: New York, 1980.

(61) Berne, B. J.; Borkovec, M.; Straub, J. Classical and modern methods in reaction rate theory. *J. Phys. Chem.* **1988**, *92*, 3711–3725.

(62) Kim, H. B.; Kitamura, N.; Kawanishi, Y.; Tazuke, S. Bell-shaped temperature dependence in quenching of excited Ru(bpy)32+ by an organic acceptor. *J. Am. Chem. Soc.* **1987**, *109*, 2506–2508.

(63) Heitele, H.; Finckh, P.; Weeren, S.; Pollinger, F.; Michel-Beyerle, M. E. Solvent polarity effects on intramolecular electron transfer. 1. Energetic aspects. *J. Phys. Chem.* **1989**, *93*, 5173–5179.

(64) Khundkar, L. R.; Perry, J. W.; Hanson, J. E. Weak temperature dependence of electron transfer rates in fixed-distance porphyrin-quinone model systems. *J. Am. Chem. Soc.* **1994**, *116*, 9700–9709.

(65) Braddock, J. N.; Meyer, T. J. Kinetics of the oxidation of $Fe(H_2O)_6^{2+}$ by polypyridine complex Ruthenium(III). Negative enthalpies of activation. *J. Am. Chem. Soc.* **1973**, *95*, 3158–3162.

(66) Cramer, J. L.; Meyer, T. J. Unusual activation parameters in the oxidation of hexaaquairon(2+) ion by polypyridine complexes of iron(III). Evidence for multiple paths for outer-sphere electron transfer. *Inorg. Chem.* **1974**, *13*, 1250–1252.

(67) Marcus, R. A.; Sutin, N. Electron-transfer reactions with unusual activation parameters. Treatment of reactions accompanied by large entropy decreases. *Inorg. Chem.* **1975**, *14*, 213–216.

(68) Matyushov, D. V.; Schmid, R. Reorganization energy of electron transfer in polar liquids: Dependence on the reactant size, temperature, and pressure. *Chem. Phys. Lett.* **1994**, *220*, 359–364.

(69) Kaduk, B.; Kowalczyk, T.; Van Voorhis, T. Constrained Density Functional Theory. *Chem. Rev.* **2012**, *112*, 321–370.

(70) Honig, B.; Sharp, K.; Yang, A. S. Macroscopic models of aqueous solutions: biological and chemical applications. *J. Phys. Chem.* **1993**, *97*, 1101–1109.

(71) Rocchia, W.; Sridharan, S.; Nicholls, A.; Alexov, E.; Chiabrera, A.; Honig, B. Rapid grid-based construction of the molecular surface and the use of induced surface charge to calculate reaction field energies: Applications to the molecular systems and geometric objects. *J. Comp. Chem.* **2002**, *23*, 128–137.

(72) Hagfeldt, A.; Grätzel, M. Molecular Photovoltaics. *Acc. Chem. Res.* **2000**, *33*, 269–277.

(73) Gust, D.; Moore, T. A.; Moore, A. L. Solar Fuels via Artificial Photosynthesis. *Acc. Chem. Res.* **2009**, *42*, 1890–1898.

(74) Guldi, D. M.; Rahman, G. M. A.; Sgobba, V.; Ehli, C. Multifunctional molecular carbon materials—from fullerenes to carbon nanotubes. *Chem. Soc. Rev.* **2006**, *35*, 471–487.

(75) Fukuzumi, S.; Ohkubo, K.; Suenobu, T. Long-Lived Charge Separation and Applications in Artificial Photosynthesis. *Acc. Chem. Res.* **2014**, *47*, 1455–1464.

(76) Imahori, H.; Tkachenko, N. V.; Vehmanen, V.; Tamaki, K.; Lemmetynen, H.; Sakata, Y.; Fukuzumi, S. An extremely small reorganization energy of electron transfer in porphyrin-fullerene dyads. *J. Phys. Chem. A* **2001**, *105*, 1750–1756.

(77) Imahori, H.; Yamada, H.; Guldi, D. M.; Endo, Y.; Shimomura, A.; Kundu, S.; Yamada, K.; Okada, T.; Sakata, Y.; Fukuzumi, S. Comparison of Reorganization Energies for Intra- and Intermolecular Electron Transfer. *Angew. Chem. Int. Ed.* **2002**, *41*, 2344–2347.

(78) D'Souza, F.; Chitta, R.; Ohkubo, K.; Tasior, M.; Subbaiyan, N. K.; Zandler, M. E.; Rogacki, M. K.; Gryko, D. T.; Fukuzumi, S. Corrole-Fullerene Dyads: Formation of Long-Lived Charge-Separated States in Nonpolar Solvents. *J. Am. Chem. Soc.* **2008**, *130*, 14263–14272.

Graphical TOC Entry